Submitted for publication in Fuel
October, 2012

Technical applicability of low-swirl fuel nozzle for liquid-fueled industrial gas turbine combustor

Masamichi Koyama[a] and Shigeru Tachibana[b]

a. Niigata Power Systems Co., Ltd., GT Development Design & Development Engineering & Technology Center, 5-2756-3 Higashiko, Seirou-machi, Kitakanbara-gun, Niigata 957-0101, Japan. Email: koyamama@niigata-power.com

b. Aerospace Research and Development Directorate, Japan Aerospace Exploration Agency, 7-44-1 Jindaiji-Higashii, Chofu, Tokyo 182-8522, Japan. Email: tachibana.shigeru@jaxa.jp

ABSTRACT

In this study, potentials of the liquid-fueled low-swirl burner technique for industrial gas-turbine combustor application are reported for the first time. A low-swirl fuel nozzle, which is a new implementation of the basic low-swirl burner design, is configured by the velocity measurement of methane-air open flames under atmospheric pressure and a low velocity (~3 m/s) condition. Flow properties, such as the axial stretch rate and virtual origins, are compared with the previously reported values with the axial vane type low-swirl injector, and it is confirmed that the flow field generated from the current implementation is of the typical low-swirl flow. Then, it is shown that the configuration successfully stabilize the lifted flame under much higher velocity (~50m/s) condition with kerosene fuel injected by a typical pressure atomizer. Finally, the fuel nozzle is installed in a 290 kW simple-cycle liquid-fueled gas turbine engine and is found to be operable over the entire operating range. The combustor inlet wall temperatures are shown to be within an acceptable range, even without the cooling air that was required for conventional combustors. This is an advantage of the lifted flame stabilized by the low-swirl technique. Although our focus is not on low emissions characteristics, NOx emissions is also found to be below maximum levels of current Japanese regulations (<84 ppm@15% O2). In sum, the proposed fuel nozzle design shows promise for the application of liquid-fueled industrial gas turbine engines.

1 INTRODUCTION

Gas turbine engines for standby generators generally use liquid hydrocarbon fuels due to their robust, rapid engine startups capability. In these gas turbines, burning of the liquid hydrocarbon fuel spray often results in significant heat radiation from the flames that can occasionally damage the fuel nozzle and/or combustor wall.

Overheating can also corrode the combustor wall surface to the extent that aggressive cooling treatments have been applied to the combustor wall of liquid-fueled gas turbine engines. For example, the systems developed by Niigata Power Systems [1-3], use cooling air supplied to the heated region to prevent over-heating. While this provision improves the durability of hot parts and extends maintenance cycles, it has several disadvantages, including lower engine efficiency and unburned hydrocarbon emissions. Thus, preventing over-heating with less or no cooling air would generate a critical advantage, as well as reducing emissions of pollutants such as NOx and soot.

This study examines the adaptation of the low-swirl burner technology, developed for ultralow emissions gas-fuel combustors (<5 ppm NOx and CO), to a liquid-fueled industrial gas turbine combustor. The low-swirl burner was developed at the Lawrence Berkeley National Laboratory [4, 5] for lean premixed combustion of gaseous fuels. It has been widely adopted for fundamental studies, since this burner generates a detached flame that is a close approximation of a freely propagating planar turbulent premixed flame. The flame configuration is considered the most fundamental for elucidating basic turbulent flame processes. From a practical perspective, many studies have been devoted to the adaptation of the technology to gas turbines. Flow field and emissions characteristics have been reported for various gaseous fuels, including natural gas, hydrogen, and syngas [6-8]. Testing of a prototype low-swirl injector for a 7MW gas turbine showed that the absence of heating of the nozzle tip due to the detached flame to be an attribute of this technology in addition to its ultra-low emissions capability[9].

To date, there has yet to be data published on burning liquid fuels with the low-swirl burner. For liquid-fueled combustors, the fuel atomization and evaporation processes, as well as the mixing process, play key roles in controlling combustion characteristics such as flame stability, flame size and pollutant emissions. Because the low-swirl burner was intended for gaseous fuel, for it to burn liquid fuels a fuel atomization and mixing system needs to be included in the design scheme. The goal of this study is to investigate the feasibility of a liquid-fueled low-swirl combustion system for gas turbine. Our approach is to integrate a simple hollow-cone type fuel atomizer into the basic low-swirl burner configuration.

The low-swirl burner principle is based on stabilization of a turbulent premixed flame in a non-recirculating divergent flow. For gas turbines, the swirler shown in Fig. 1(a) has been developed to produce a divergent flow in the combustor. The main difference between this swirler and those of conventional high-swirl design is the opening of a center channel through which a portion of the flow of reactants bypasses the swirl annulus. When the flow of reactants discharges into the combustor, the transverse gradient induced by the centrifugal forces of the swirling flow causes the

center non-swirling flow to diverge. Flow recirculation is avoided because the un-swirled center flow inhibits the propensity of its surrounding swirling flow to cause vortex breakdown. For a given swirler geometry, the rate of flow divergence it generates is controlled by the mass ratio of the swirled and unswirled flows. This ratio, also called flow split, can be varied by covering the center channel with a perforated plate. Because the interaction between the unswirled and swirled flow is a critical process, the low-swirl injectors developed for gaseous fueled gas turbines are fitted with small injection spokes upstream of the swirler to minimize the disturbance of the flow feeding into the swirler [9]. In adaptation to liquid fuel, a top issue is whether or not the liquid fuel atomizer can be fitted in the flow path without causing significant disruption of the divergent flow formation. Other significant issues are associated with optimizing the rates of fuel vaporization and mixing so to enable a flame in the combustor to burn in a partial or full prevaporized-premixed combustion mode. Once these design issues are addressed, performance parameters such as flame stability, turndown, and emissions can then be evaluated to access the feasibility of adapting low-swirl burners to liquid fueled gas turbines.

The experimental test series is divided into three phases to address the issues outlined above. First, we performed PIV measurements to verify that our new implementation of a low-swirl burner fitted with a fuel atomizer produces flow pattern that has the low-swirl divergent flow characteristics. Premixed gaseous flames were used in this phase of our development. The experiments also include a study on the effects of nozzle tip shape on flow patterns by comparing axial velocity profiles along the center line. Second, atmospheric combustion testing using kerosene is performed with a single-can type combustor to determine if the burner is capable of generating a lifted flame inside the confinement of a combustor. We observed the flames through a window located on the side wall of the combustion chamber. Finally, engine test is performed to confirm the technical applicability of the liquid-fueled low-swirl combustion concept for gas turbines. The engine testbed was a 290 kW simple-cycle liquid-fueled gas turbine engine. Wall temperatures on the combustor face plate are measured under several load conditions.

2 LAYOUT OF A LOW-SWIRL BURNER WITH LIQUID-FUEL NOZZLE

Fig.1 (b) shows the design of the low-swirl burner that we developed for operating with liquid fuel. It is sized to fit the combustor of the 290kW gas turbine. The fuel nozzle is mounted at the center of the perforated plate (78% blockage) covering the center channel whose diameter is 80% of the nozzle diameter. Unlike the design shown in Fig.1 (a), the inlet of the outer annulus of the nozzle is plugged by a ring plate. Instead of swirl vanes, multiple orifices pass tangentially through the outer cylindrical wall are used to impart swirling motion. There are 16 orifices of

diameter φ=5mm (2 rows of 8 orifices with a pitch of 10 mm along the axial direction) and 40 orifices of φ=8 mm (5 rows of 8 orifices with a pitch of 10 mm along the axial direction) from upstream to downstream. This design is essentially a hybrid of the swirl-jet and swirl-vane configurations reported in previous publications (e.g. [10, 8]). The swirl number of our low-swirl burner can be adjusted by changing the combination of the blockage ratio of the perforated plate and also by the number of tangential orifices to produce a stable lifted flame. We choose this configuration precisely for the flexibility it gives in adjusting the swirl number for exploring the operating regimes for firing with liquid fuels.

We derived a geometric swirl number for this nozzle the same way as in previous literatures (e.g. [11]) by omitting the pressure term from the original definition [12] and assuming plug flow conditions for the cross-sections of the axial and tangential flow passages to be as Eq. (1):

$$S_g = \frac{G_\phi}{R_2 G_x} = \frac{2\pi(1-R^3)R_1^2}{3A_\phi\left(M^2(1-R^2)+R^2\right)} \quad . \tag{1}$$

Here, G_ϕ is the axial flux of angular momentum; G_x the axial flux of linear momentum; M the ratio of the mass flow rate through the inner tube to the mass flow rate through the tangential orifices; R the ratio of inner tube radius R1, to outer tube radius R_2 in the C-C cross section in Fig.1; and A_ϕ the x-r cross-sectional area of the tangential flow passage (the circular channel between the inner and outer tubes). Substituting the numerical values of the current nozzle provides the geometrical swirl number S_g = 0.50. As described above, there are several critical assumptions for deriving the swirl number. Thus, one should treat this number as a design parameter rather than as the actual flow property.

3 CONCEPT VERIFICATION WITH PREMIXED GAS COMBUSTION

The goal of the PIV measurements is to determine if the nozzle generates a flow field that is comparable to those of the low-swirl burner for gaseous fuels. For this purpose, a bluff body is installed as a surrogate of the liquid fuel atomizer (Fig.1) to simulate its blockage. A methane-air gas mixture is supplied to the cylindrical chamber (Fig.2 (a)) which represents an idealized premixed condition without involving atomization and mixing processes. The obtained flow characteristics can then be compared directly with those reported in previous studies. In addition, PIV experiments were performed using three types of nozzle tips as shown in Fig.2(a). One type has a sharp edge (C0). The other types have chamfers with radii of 3 and 8 mm, denoted C3 and C8, respectively.

3.1 PIV measurement setup

Fig.2 (a) shows the configuration of the test rig. Methane and air are well-mixed with a static mixer placed before entering the cylindrical chamber. The flow rate for the mixture is 990 L/min, which corresponds to a nozzle bulk flow velocity of 3 m/s. The equivalence ratio, in the reacting case, is 0.80. As can be seen, this low-swirl burner with a surrogate fuel nozzle generates a lifted flame in a semi-infinite space as shown in Fig.2 (b).

The PIV system is composed of a double-pulse Nd:YAG laser (New Wave Gemini PIV), a synchronizer, a CCD camera (TSI, PIVCAM 10-30, 1k x 1k pixels) with a lens and optical filter. SiO2 particles with a typical diameter of 4 microns were used as seeding particles. The field of view is 80 mm x 80 mm. Vector calculations were done using the DaVis software (LaVision). We used the cross-correlation method with a multi-pass iteration mode (from 64 x 64 to 32 x 32 pixels) and performed a validation with a peak ratio factor of 2.

3.2 Results of PIV measurement

Fig.3 and 4, respectively, show 2D vector flow fields for cold flow and reacting flow. From top to bottom, the three figures in each case are for nozzle tip types C0, C3, and C8. In the cold flow cases (Fig.3), the radial flow discharge angles are very shallow, and axial velocity decay rates along the axial direction are small. The flow has a slightly non-axisymmetric distribution, as can be identified by the relatively low-speed zone in the off-center range of -20 mm < r < 0 mm and the high-speed zone in the range r > 20 mm. We suspect this is due to the low Re number condition, especially at low bulk flow velocity, as observed in the flame structure for lower velocity conditions in a previous study [13]. The non-axisymmetric feature can be due to a slight geometric variation such as the misalignment of the perforated plate. Ref [13] also shows that more uniform flow distribution is achieved when the effect of turbulence is increased at higher flow velocities. In the cases of reacting flow (Fig.4), the presence of the flame increases the radial flow discharge angles, resulting in faster decay of the axial velocity of the unburnt gas along the axial direction. Higher velocity is observed due to gas expansion downstream. Increasing the chamfer dimension from C0 to C8 appeared to shift the flow field along the axial direction. Larger chamfer dimensions pulled the divergent flow structure upstream. This feature can be accessed by looking at the axial velocity profiles along the central axis.

Fig.5 (a) and (b) show the velocity profiles at r=0 and -15mm locations, respectively. The off-centered location, r=-15mm, is corresponding to the location where axial velocity shows the minimum value due to the non-axisymmetric feature mentioned above. The velocity profiles in the cold flow cases indicated low decay rates. In the cases of reacting flow, the presence of the flame increased decay rates. Gas expansion resulted in positive slope values after the

flame leading-edge positions. In both the cold and reacting flow cases, no recirculation zone was observed. As described earlier, the weak swirl adds centrifugal force on the core axial jet flow, which results in generating divergent flows. These flow characteristics are representative of low-swirl combustion flow [5, 6]. Note that the flame leading-edge position, defined as the point just upstream of the minimum velocity position, shifts, depending on the nozzle tip shape. The flame lift-off height decreased with greater chamfer dimensions. The lift-off heights were approximately 38, 34, and 29 mm (33, 32 and 25 mm) for C0, C3, and C8, respectively, at r = 0 mm (r = -15mm) location. The velocity profiles, represented by negative and positive slopes, were similar for different nozzle tips. Only the axial position of the profile appeared to be affected by chamfer dimensions. To confirm this, we plotted the normalized velocity profiles in cases of reacting flow against the virtual origins (Fig.6). The bulk velocity U0 =3m/s is used for normalization. The virtual origins are determined by linear fitting of the velocity profiles in the linear decaying range. Linear fitting provided the values for the axial stretch rate (or decay rate) -0.010 to -0.009 (1/mm) for r = 0 mm (-0.013 (1/mm) for r = -15mm) , which are somewhat lower than the previously reported value of -0.017 (1/mm) for the vane-type low-swirl injector [6]. This may be due to the fact that the flowfield is underdeveloped at a bulk flow velocity of 3 m/s. The linear fits of the axial velocity profile also provided the values x0 = -21, -23, and -30 mm (-16, -19, and -27 mm) for C0, C3, and C8, respectively, at r = 0 mm (r = -15 mm). These values are comparable to the values given in the literature [6]. The profiles in Fig.6 are mutually consistent. This means chamfer dimensions primarily affect the axial position of the flame while other flow characteristics, including global stretch rate are unaffected. This suggests that we can control the flame lift-off position simply by changing chamfer dimensions. This is a key technical advantage, since controlling this factor will attenuate nozzle overheating.

4 ATMOSPHERIC COMBUSTION TEST WITH LIQUID FUEL

4.1 Test rig configurations

Fig.7 is a schematic of the atmospheric combustion test system. Flow of air from an electric blower is divided into pre-heat and test sections. The test air is preheated with a heat exchanger before being supplied to the test section. The bulk flow velocity at the nozzle exit is 48 m/s, which is comparable to the real gas-turbine conditions. Fig.8 gives a more detailed view of the test section. The fuel nozzle was mounted on the face plate of the combustor. It has a nozzle tip type C8 with hollow-cone fuel atomizer installed at the inlet. Fig.9 shows the details of the atomizer tip, which has two fuel supplies: Line A and Line B. In the case of low flow rates, fuel is fed into a swirl chamber through the tangential ports of Line A only. In this case, Line B is closed. Under high flow rate conditions, fuel is supplied through

both Line A and Line B. We selected the former in the atmospheric combustion tests. Except for the use of a fuel atomizer instead of its surrogate, the geometry of the nozzle was identical to the one used in the PIV measurement. No cooling air was fed through the face plate. The flames can be observed through a glass window on the side wall (Fig.8). Temperatures on the face plate are measured via thermocouples attached to the back surface of the face plate at three locations: T1, T2, and T3 (Fig.8). Table 1 gives the test conditions. The fuel was kerosene; the nozzle tip type was C8. We chose C8 type nozzle tip for the atmospheric combustion and engine tests because it showed the best performance of lean blowout limits among the three types.

4.2 Results of the combustion test

Fig.10 shows photographs of the flame at three fuel flow rate conditions. The flow is from right to left. It can be observed that a lifted flame was stabilized at the three test conditions. Successful firing of the liquid-fueled LSB has several significant implications. The fact that theses stable flames could be maintained means that they burn in the form of a propagating premixed turbulent flame. Therefore, the fuel nozzle is capable of generating a flow of reactants at the nozzle exit that is sufficiently prevaporized and premixed to support propagating flame behavior. The flame lift off positions, as shown in Fig 10, are also consistent with the lift off position of the CH_4 flame in Fig. 2(b). From previous flowfield analysis, it has been shown that the flame position of the low-swirl burner remains unchanged throughout a wide range of bulk velocities due to a linear coupling between the self-similar characteristics of the divergent flow and a linear correlation of the local turbulent displacement flame speed with turbulence intensity. The consistency of the positions of the liquid-fuels flames at 48 m/s and the CH_4 flames at 3 m/s means that the flow field generated by the current low-swirl burner with a hybrid swirler produces a divergent flow whose self-similar behavior is the same as those of the other two versions. Even though we are uncertain about the local conditions, i.e. degree of vaporization, equivalence ratio and homogeneity of the mixture, the fact that the liquid-fueled flames are at the same position as the CH_4 flame also implies that the behavior of the local turbulent displacement flame speeds of the kerosene flames appear to be similar to that of CH_4 flames.

Fig.11 shows the combustor inlet wall temperature. As to be expected, wall temperature is higher at locations closer to the nozzle. The overall increasing trend with equivalence ratio is also consistent with the increasing flame temperature. The highest wall temperature observed is 568K. This is lower than the maximum limit of 923K for the production gas turbines. This demonstrates the potential benefit of the lifted flame to prevent overheating by heat radiation from the luminous flame. These results encouraged us to continue our tests in a gas turbine engine testbed.

5 DEMONSTRATION IN AN ENGINE

5.1 Gas turbine engine testbed

Fig.12 is a photograph of the gas turbine engine testbed. The rated output power is 290 kW. This simple cycle gas turbine engine is composed of a single-stage centrifugal compressor, a single-can combustor, and a single-stage radial turbine. Table 2 gives engine specifications.

Fig.13 compares the inlet configurations of the production and the present combustor. The production combustor has a fuel nozzle with an air-blast atomizer nested inside a dual annulus counter-swirl configuration. The atomizer and the swirler is mounted at the inlet of the mixing tube shown in Fig.13 (a). The face plate of the production combustor, as shown in the lower part of Fig 13(a) has an intricate array of orifices for cooling. Air jets generated by these orifices cool the heat shield. In contrast, the present combustor inlet is much simpler consisting of a flat disk with the low-swirl burner mounted in the middle (Fig.13 (b)). No cooling air is supplied through the face plate. This configuration when proven to be operational, can bring about reductions of the costs in manufacturing of the combustor and its life-cycle maintenance.

5.2 Results of the engine test

Although the fuel atomizer used in the engine testbed is the same as in the atmospheric combustion test, due to increase fuel flow rates for the high pressure engine conditions fuel is fed through Line A and Line B. The tests with the low-swirl burner were conducted using the same ignition system and light-off sequence as our production combustor. Ease of lighting of the low-swirl burner with our ignitor was found to be same as the production combustor by changing only the axial position of the ignitor. Upon light-off, the loading characteristics of the low-swirl burner were found to be the same as the production combustor. The testbed engine with the low-swirl combustor was evaluated at four load points covering a 2:1 turndown range. We measured temperatures at the three locations in the combustor and the results are compared with those from a production combustor in Fig.14. Despite the absence of cooling air, the inlet wall for the present combustor wall temperatures were lower than in a production air-cooled combustor at all three locations. At peak load, the reduction in wall temperature is between 200 to 300K. The maximum wall temperature for the present combustor was 693K (200 kW load and T”1 location). This is well below the in-house maximum limit of 923K for safe engine operation. These tests results not only demonstrate the feasibility of the low-swirl combustor for operating in a liquid-fuel gas turbine, they also show its potential to preventing overheating of the combustor wall.

Although the low-swirl combustor was not optimized for low emissions performance, we performed gas sampling measurements of NOx and CO for future reference. Fig.15 shows the emissions at four conditions between half (150 kW) and full load (290 kW). Solid and dashed lines show NOx and CO, respectively. NOx emissions were 10-60 ppm lower than for the production combustor under the same load conditions. An encouraging aspect is the emission levels for the low-swirl combustor meet current emissions standards in Japan (<84 ppm@15% O2). However, CO emissions showed much higher values compared to the production combustor, which implied the lower NOx emissions were coming from incomplete combustion. In this fuel nozzle, fuel was only injected at the center, therefore, the dilution in the outer edge of the flame may contribute to incomplete combustion and thus increment of CO. Further examination of these aspects should be addressed for improving NOx performance to meet more stringent future regulations in the future study.

6 DISCUSSION

6.1 Characterizing flow field development

The bulk flow velocity condition in the PIV test of this study was limited to 3m/s, which is relatively low and the results cannot be used to confirm the self-similarity of the flow field as discussed in Appendix A of Ref [13]. This is due to the relatively large diameter of the nozzle and the low capacity of the laboratory air supply. At lower velocity conditions, the effects of laminar flame speed are nonnegligible. Additionally, sensitivity to nozzle design, including alignments of the perforated plate orifices and swirl orifices, is pronounced at lower velocities. Higher velocities diminish these effects. Thus, even though the velocity field of the present nozzle showed features similar to those of the low-swirl injectors reported in previous studies, further study of flow characteristics for higher velocities is needed to identify the characteristics specific to this nozzle geometry. Additionally, the present nozzle configuration is more similar to the jet-LSB than the vane-LSI. The jet-LSB data showed deviations from the linear turbulent flame speed correlation [6]. This may also occur with this nozzle. Though the flame positions of the methane flame at 3 m/s and the kerosene fueled flame implied that some form of self-similar behavior could have been achieved, it is of significance to verify by more experiments. This is because the axial momentum generated by the fuel atomizer is not present in the methane tests. The interplay between the fuel atomizer flow and the low-swirl burner flow needs to be included in the analysis. Once flow similarity characteristic for this type of nozzle is acquired, we can apply this knowledge to advance other engine combustor developments.

The presence of the fuel atomizer acting as a bluff body makes it impossible to avoid the generation of a recirculation zone in its wake. This may lead to premature flashbacks as observed in some type of conventional combustors [14]. The fact that no flashback was observed in our test suggests that the fuel spray axial momentum may have prevented or mitigated the recirculation zone. If this can be verified by experiments, this would be another potential attribute of the low-swirl injector.

6.2 Improving emissions

Our study has fulfilled our goals to confirm the validity of low-swirl flame stabilization with liquid fuel and to demonstrate the effectiveness of this approach in preventing overheating. To continue the development, the logical next step is to improve gas emissions characteristics. Though we found that NOx emissions were lower than the standard in Japan we also observed that CO emissions were relatively high at full load operation (~260 ppm). Definitely, this point should be addressed in the future study. The present study utilized a single fuel pressure atomizer that supplied fuel to the central region of the low-swirl burner. Because no fuel was injected in the swirl annulus, there was insufficient fuel air mixing to ensure uniform burning and to provide good emissions performance. One possible solution is staged fuel injectors combined with air-blast fuel atomizers. The main challenge in staging is that most air-blast atomizers deploy a multi-swirl configuration to generate strong shear flow. Strong shear flow is preferable for atomization performance, but less suitable from the perspective of a low-swirl flow field, in particular, in the core jet and the swirl flow regions. This aspect will require innovative solutions.

The diameter ratio and flow split between the inner and outer (swirl) channel are another key design parameters to optimize air-to-fuel ratio. A parametric study was reported recently for the vane-type LSI [16]. This kind of parametric study helps a lot to have a useful design guideline for developing a low-emission jet-type LSB as well.

Even though we have not experienced combustion instabilities in this test series, one may have to resolve the instability problems when operating under fuel lean conditions. Our future work will also examine the use of other liquid fuels, including heavy oil and waste solvent. The heat radiation from the combustion of such fuels tends to be stronger than for kerosene, and lifted flame stabilization should prove more effective.

7 CONCLUSION

Three sets of combustion experiments on a new implementation of the low-swirl type fuel nozzle were performed to investigate its applicability to a liquid-fueled industrial gas turbine.

Atmospheric PIV tests at a low bulk flow velocity of 3 m/s were performed to compare the flow characteristics of the new fuel nozzle to those observed in the low-swirl injector flows reported in previous studies. It was found that the current low-swirl fuel nozzle produces the same divergent flow structures as previous designs. In addition, we found that chamfer dimensions of the nozzle tip primarily affected the axial shift of the divergent velocity profile, which in turn determines the flame leading-edge position while keeping other flow characteristics unchanged. This is one of the our key findings, since controlling the proximity of the flame to the faceplate will provide a means to control nozzle overheating.

To verify liquid-fuel operation, a hollow-cone fuel atomizer was mounted at the center of the nozzle and tested at standard atmosphere with kerosene at a realistic bulk flow velocity of 48m/s.It was observed that lifted flames were stabilized across the test points that consisted of fuel lean and fuel rich conditions at 473K air preheat. Flame lift-off distances were not measured in a precise manner, but from an eye-observation through the side window, they were not sensitive to stoichiometry. Since the geometry of the nozzle is the same as the one used in the PIV tests the behaviors of the kerosene flames show them to be consistent with those of gas-fueled low-swirl flames.

The low-swirl liquid-fuel injector was mounted in a test-bed gas turbine of normally 290 kW output. The results showed that it to operate at typical conditions of 4.01 pressure ratio and 473K inlet temperature. Despite the absence of cooling air, inlet wall temperatures for the combustor with the low-swirl type fuel injector were lower at all measurement points than for a production air-cooled combustor. The peak measured temperature for the present combustor was 650K. This is sufficient for safe engine operations, suggesting the considerable promise of the present fuel nozzle geometry in preventing overheating. NOx emissions for the present combustor were 10-60 ppm below those of the production combustor under all tested load conditions. The emissions from the present combustor also met all current emissions standards in Japan. Nevertheless, additional study is needed to accommodate more stringent future regulations in the area of low emissions performance, not just for NOx but for combustion efficiency and soot. The results obtained—the wall temperature characteristics in particular—demonstrate that the proposed fuel nozzle design offers significant promise for use in industrial liquid fuel gas turbine engines.

ACKNOWLEDGMENT

The authors acknowledge Dr. Robert K. Cheng of Lawrence Berkeley National Laboratory for a highly useful discussion.

NOMENCLATURE

A_{EP} Area of the swirl flow passage in the x-r cross-plane

M Ratio of mass flow rate through inner tube to mass flow rate through swirl orifices ($M \equiv \dot{m}_x / \dot{m}_\phi$)

$\dot{m}_x$ Mass flow rate through inner tube

$\dot{m}_\phi$ Mass flow rate through swirl orifices

Q_f Fuel volume flow rate

R Ratio of inner tube radius to nozzle radius ($R=R_1 / R_2$)

R_1 Inner radius of the inner tube in C-C cross section (Fig.1)

R_2 Inner radius of the outer tube in C-C cross section (Fig.1)

r Radial distance

S_g Geometrical swirl number

U_0 Bulk flow velocity

U Axial velocity

x Axial distance from injector exit

x_0 Virtual origin of divergent flow

E.R. Equivalence ratio

φ Orifice diameter

REFERENCES

[1] Koyama M, Fujiwara H. Development of a Dual-Fuel Gas Turbine Engine of Liquid and Low-Calorific Gas. JSME Fluids and Thermal Engineering Vol.49 No.2 2006; P224-229.

[2] Yoshimura Y, Kudo Y, Ito M, Uji S. VOC Energy Recovery by Gas Turbine Cogeneration. IGTC 2007 Tokyo; TS-010.

[3] Asai H, Koyama M, Nakayama Y, Toba K. Efforts toward the Effective Use of Unused Energy by Small Gas Turbine Generators. CIMAC Congress 2007; No. 38.

[4] Chan C K, Lau K S, Chin W K, Cheng R K. Freely Propagating Open Premixed Turbulent Flames Stabilized by Swirl. Proceedings of the Combustion Institute 1992 24(1-2); pp. 511-518.

[5] Cheng R K. Velocity and Scalar Characteristics of Premixed Turbulent Flames Stabilized by Weak Swirl. Combust. Flame 1995; 101: 1-14.

[6] Cheng R K, Littlejohn D, Nazeer W A, Smith K O. Laboratory Studies of the Flow Field Characteristics of Low-Swirl Injectors for Application to Fuel-Flexible Turbines. Journal of Engineering for Gas Turbines and Power 2008; 130(2): p. 21501-21511.

[7] Cheng R K, Littlejohn D, Strakey P, Sidwell T. Laboratory Investigations of Low-Swirl Injectors with H2 and CH_4 at Gas Turbine Conditions. Proc. Comb. Inst. 2009; 32 p. 3001-3009.

[8] Littlejohn D, Cheng R K, Noble D R, Lieuwen T. Laboratory Investigations of Low-Swirl Injector Operating with Syngases. Journal of Engineering for Gas Turbines and Power 2010; 132(1): p. 011502-011510.

[9] Nazeer W A, Smith K O, Sheppard P, Cheng R K, Littlejohn D. Full Scale Testing of a Low Swirl Fuel Injector Concept for Ultra-Low NOx Gas Turbine Combustion Systems. ASME Turbo Expo 2006; GT2006-90150.

[10] Bedat B, Cheng R K. Experimental Study of Premixed Flames in Intense Isotropic Turbulence. Combustion and Flame 1995; 100(3): p. 485-494.

[11] Palies P, Durox D, Schuller T, Candel S. Experimental Study on the Effect of Swirler Geometry and Swirl Number on Flame Describing Functions. Combustion Science and Technology 2011; 183:7 704-717.

[12]Beer J M, Chigier N. Combustion Aerodynamics Applied Science Publishers 1972; London.

[13] Day M, Tachibana S, Bell J, Lijewski M, Beckner V, Cheng R K. A combined computational and experimental characterization of lean premixed turbulent low swirl laboratory flames. I. Methane flames. Combustion and Flame 2012; 159(1), 275-290.

[14] Koyama M, Fujiwara H, Zimmer L, Tachibana S. Effects of swirl combination and mixing tube geometry on combustion instabilities in a premixed combustor; ASME Turbo Expo 2006; GT2006-90891.

[15] Cheng R K, Littlejohn D, Strakey P A, Sidwell T. Laboratory investigations of a low-swirl injector with H2 and CH_4 at gas turbine conditions. Combustion Institute 2009; 32(2):3001-3009.

[16] Therkelsen P L, Littlejohn D, and Cheng R K. Parametric study of low-swirl injector geometry on its operability. ASME Turbo Expo 2012; GT2012-68436.

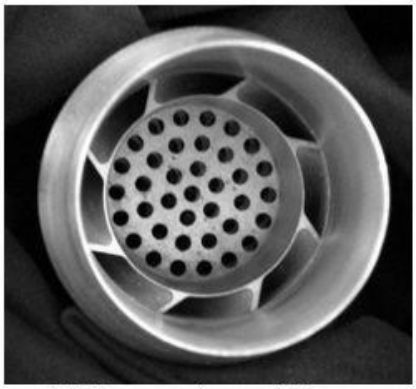

(a) Vane-type low-swirl burner

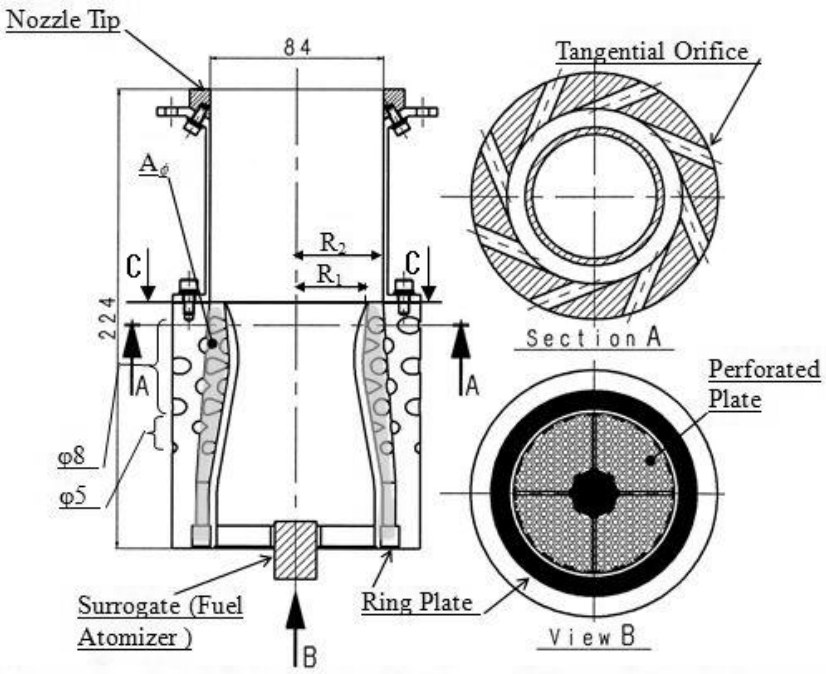

(b) Present low-swirl burner configuration with a bluff body as a surrogate of liquid fuel atomizer (for PIV purpose)

Fig. 1. (a) Vane-type low-swirl burner and (b) present low-swirl burner configurations.

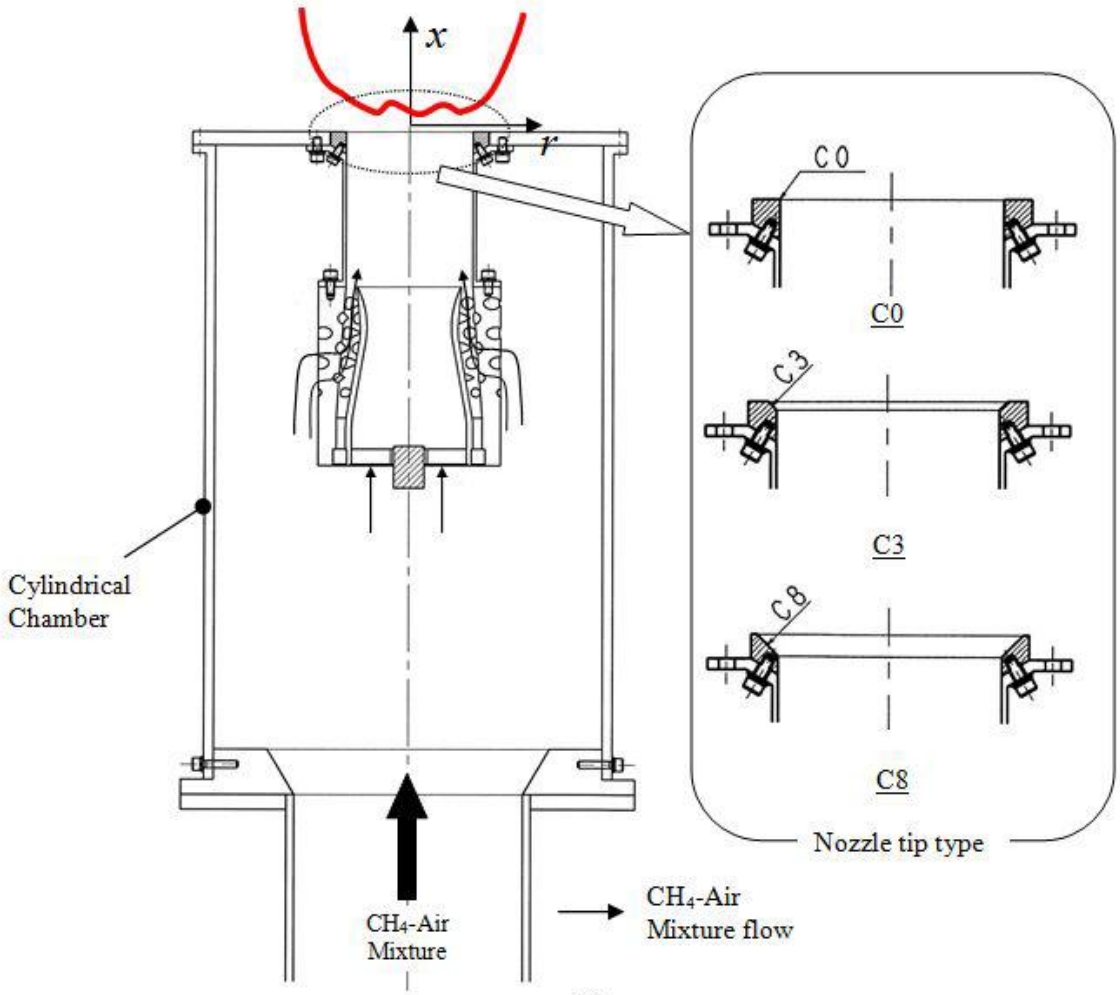

Fig. 2. (a) Test rig for PIV measurement; (b) Direct photo of flame. (the yellow in the flame is attributable to radiation from SiO_2 seeding particles.)

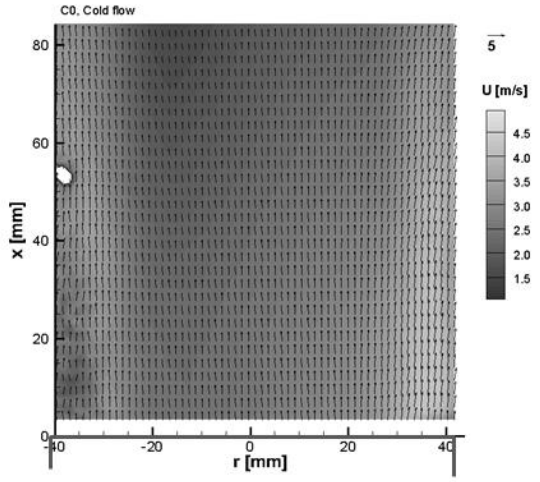

(a) C0

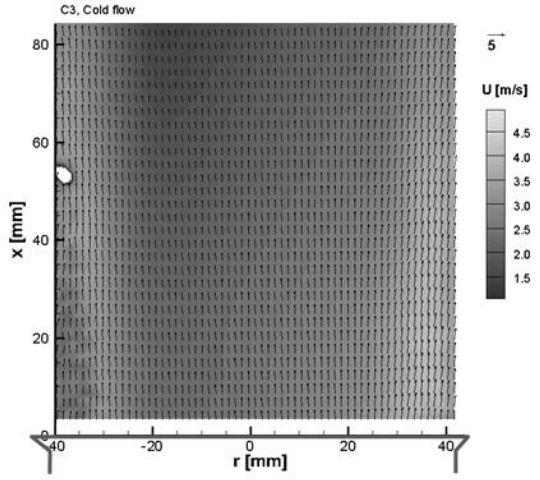

(b) C3

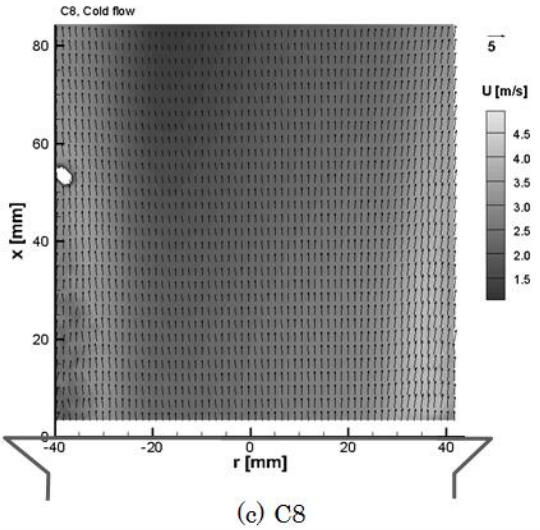

(c) C8

Fig. 3. Mean velocity profiles (cold flow) (——— : Nozzle tip shapes)

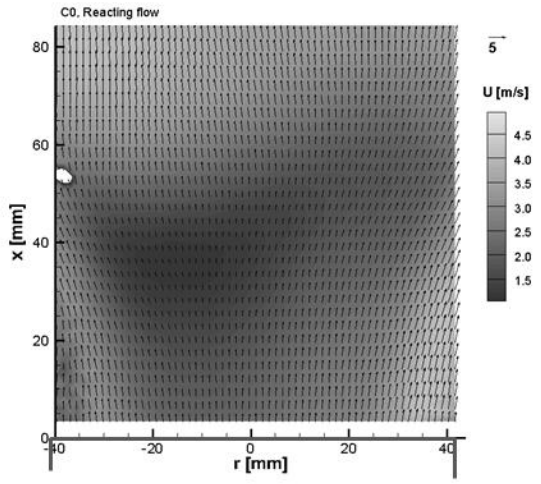

(a) C0

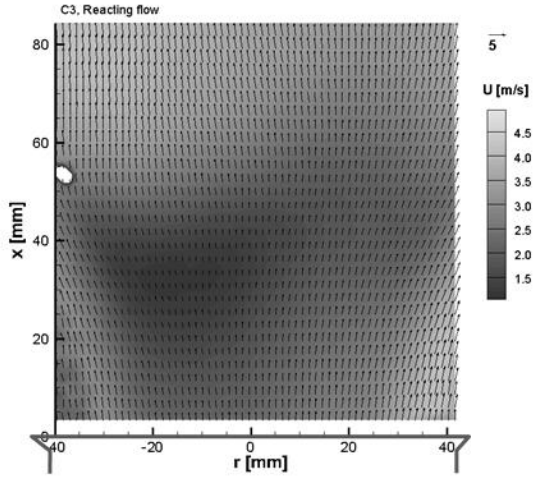

(b) C3

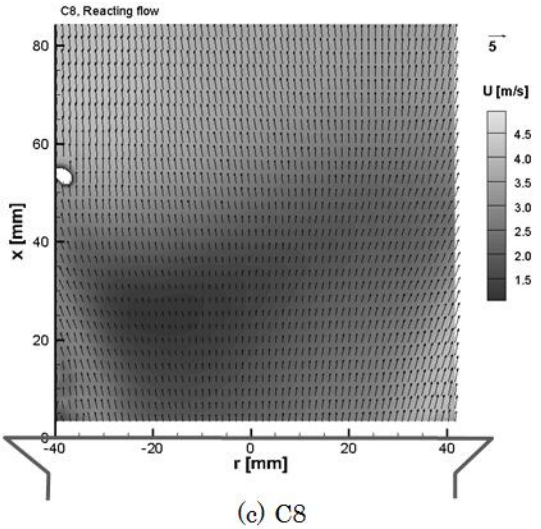

(c) C8

Fig. 4. Mean velocity profiles (reacting flow). (——— : Nozzle tip shapes)

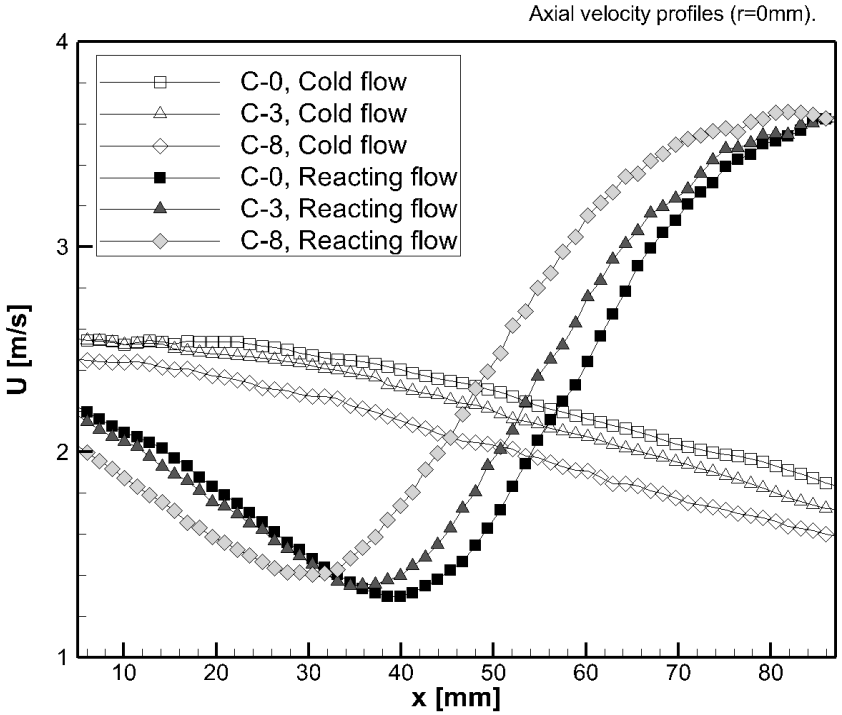

(a) r = 0mm

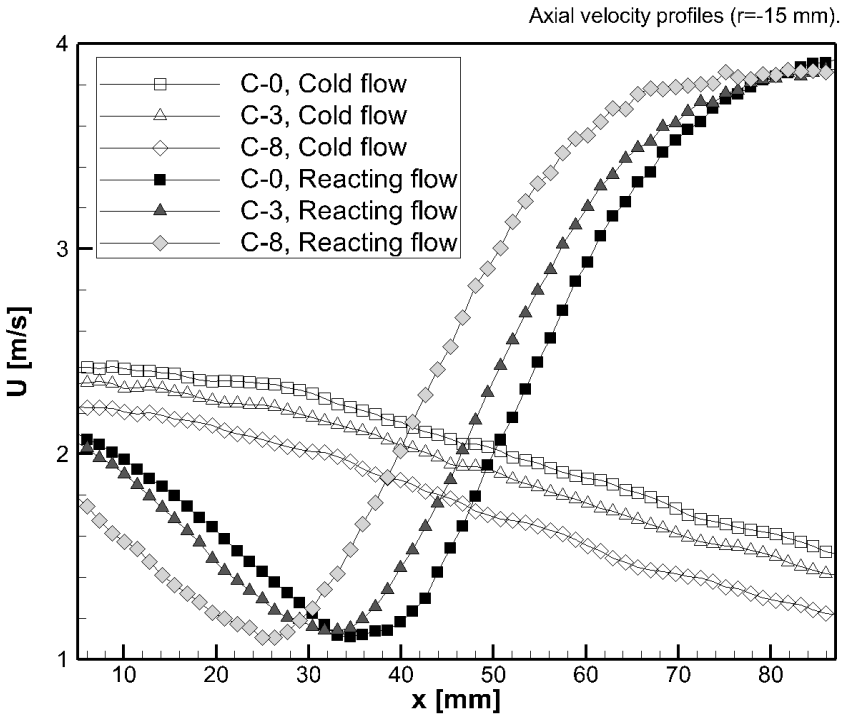

(b) r = -15mm

Fig. 5. Mean axial velocity profiles

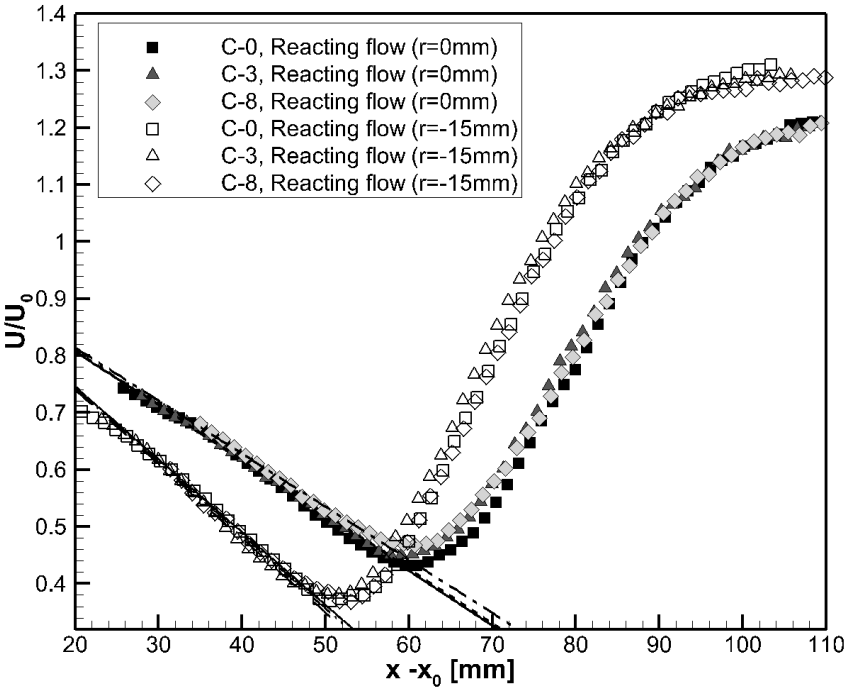

Fig. 6. Normalized mean axial velocity profiles plotted against distance from virtual origins (reacting case)

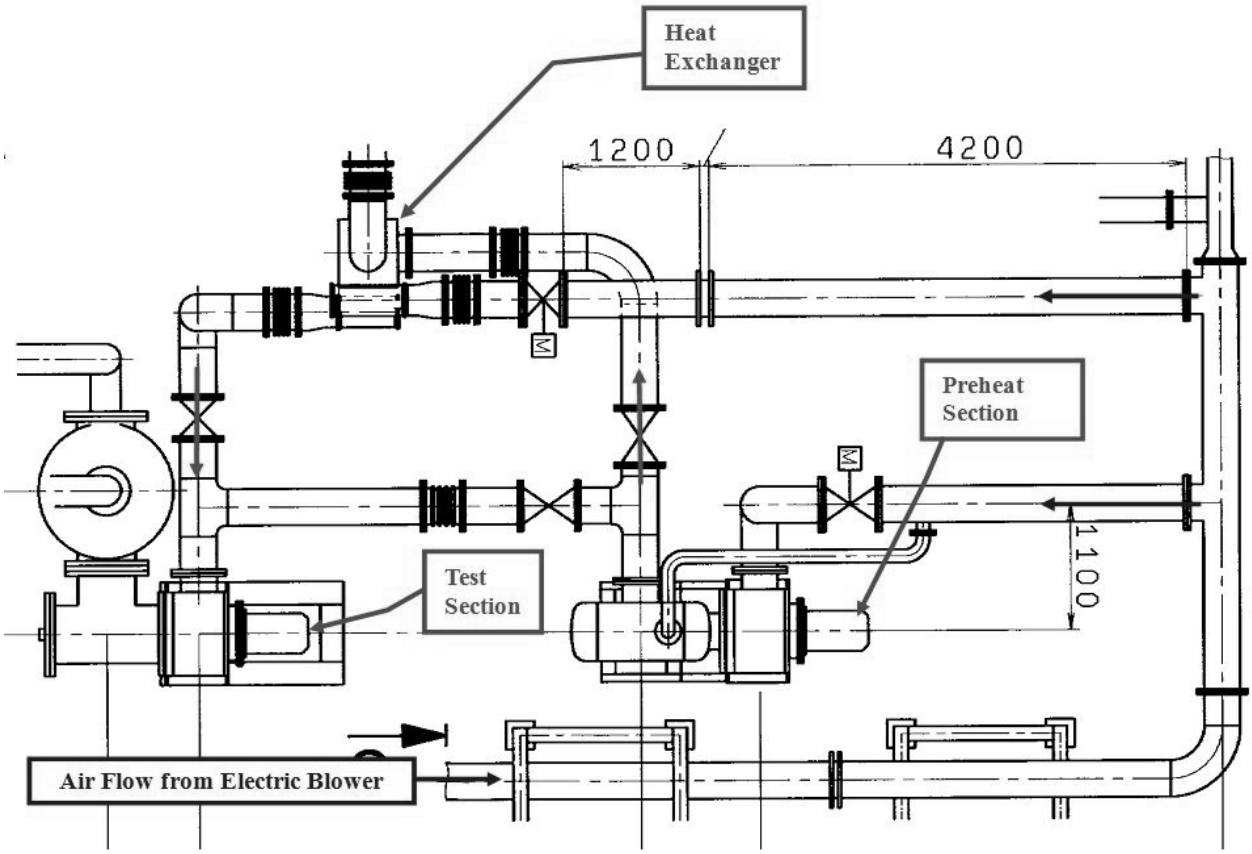

Fig. 7. Schematic of atmospheric combustion test system

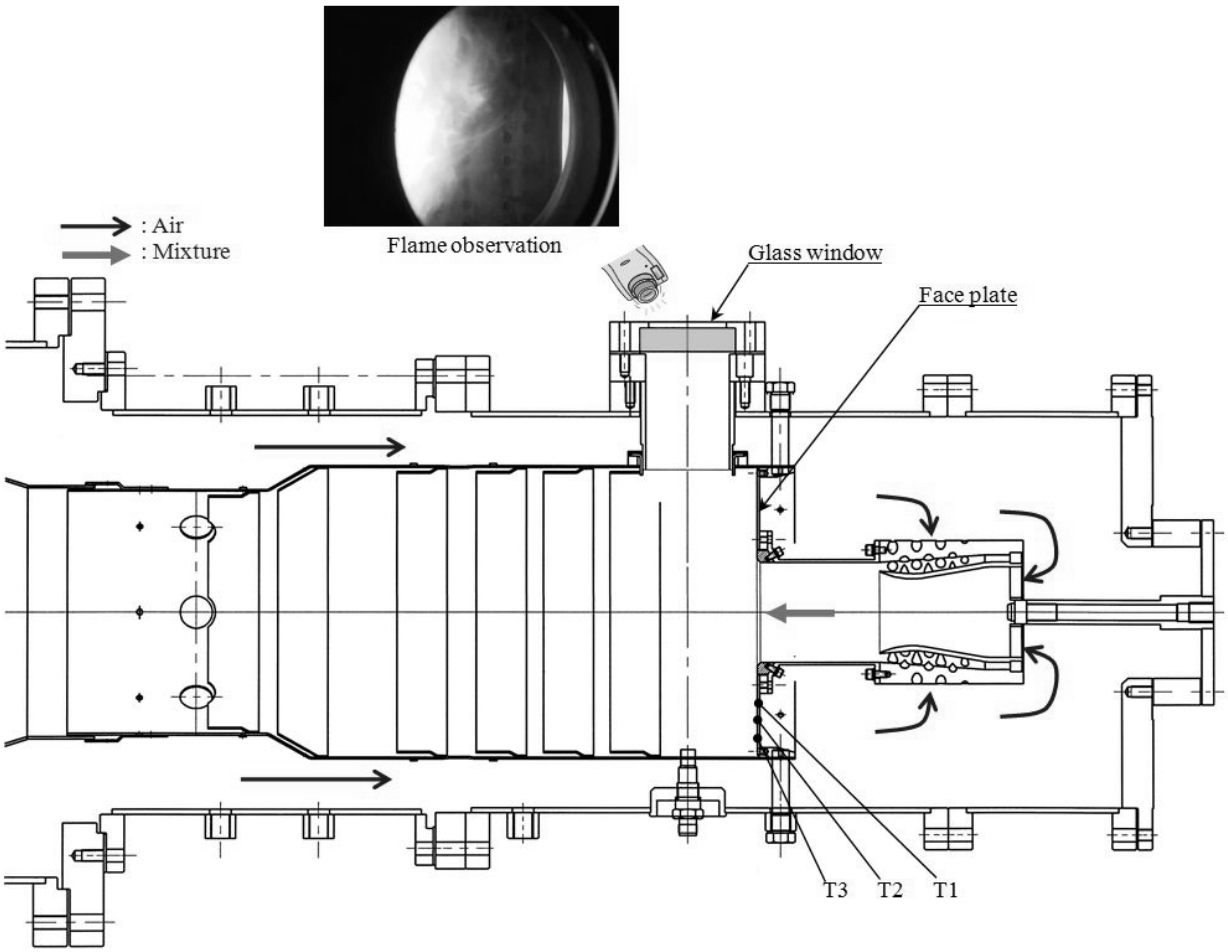

Fig. 8. Detailed view of the test section

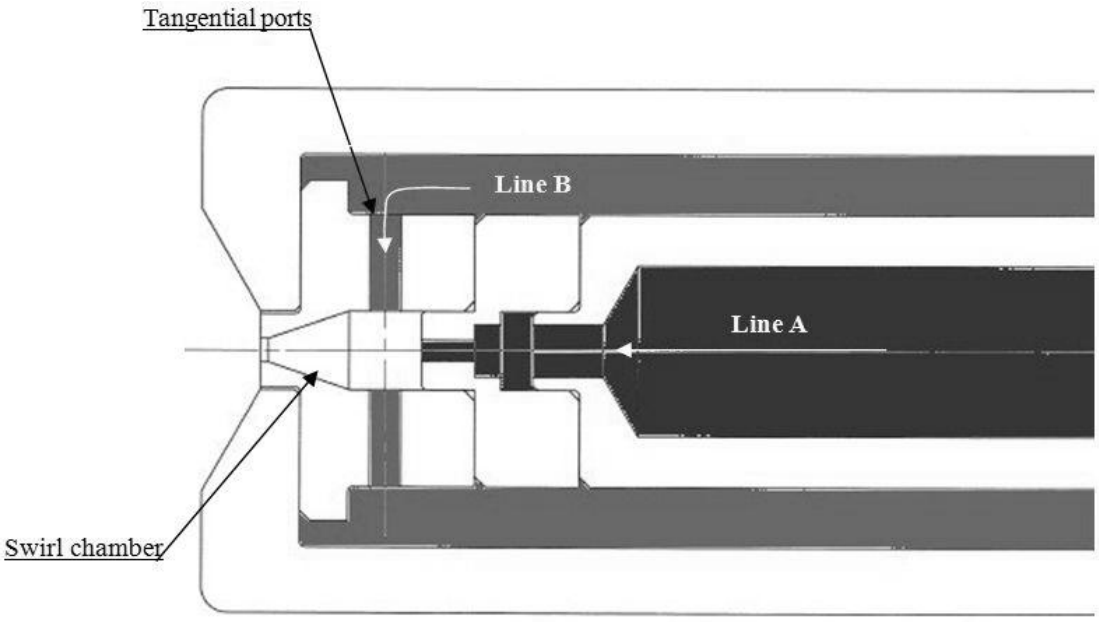

Fig. 9. Configuration of the liquid fuel atomizer

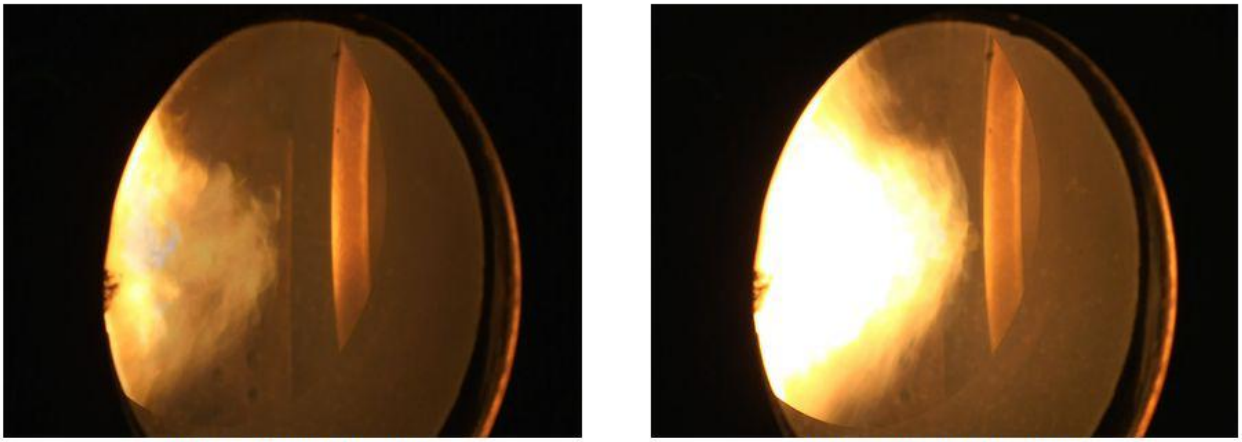

(a) E.R. (nozzle) = 0.56

(b) E.R. (nozzle) = 0.82

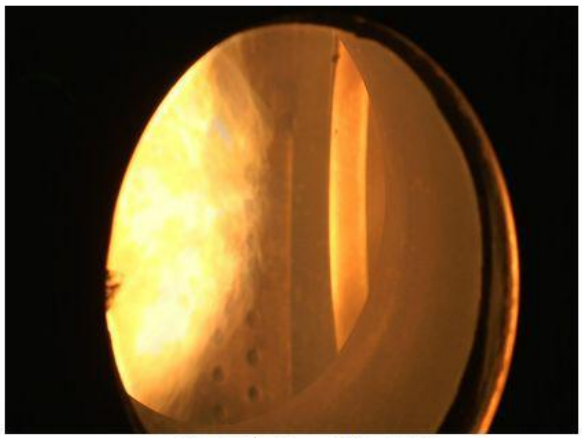

(c) E.R. (nozzle) = 1.08

Fig. 10. Flames in the atmospheric combustion test

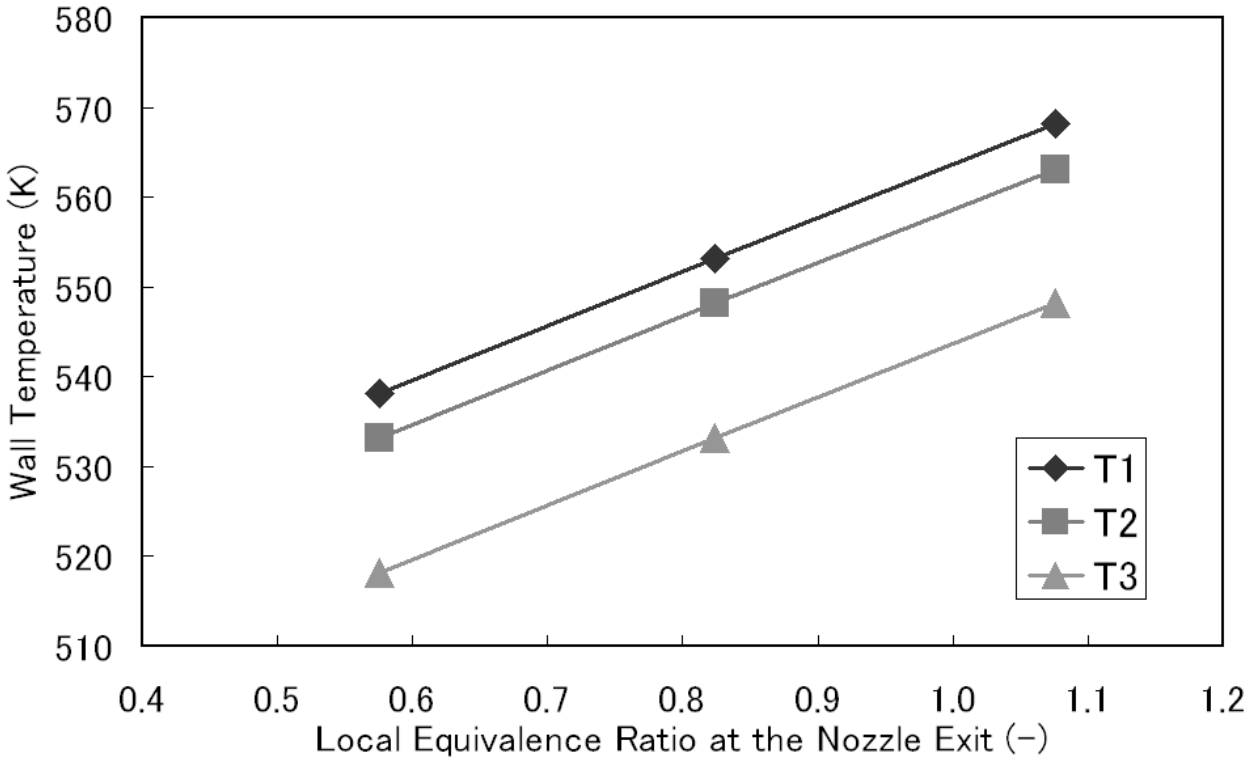

Fig. 11. Combustor inlet wall temperature in the atmospheric combustion test (the locations T1, T2, and T3 are indicated in fig.9.)

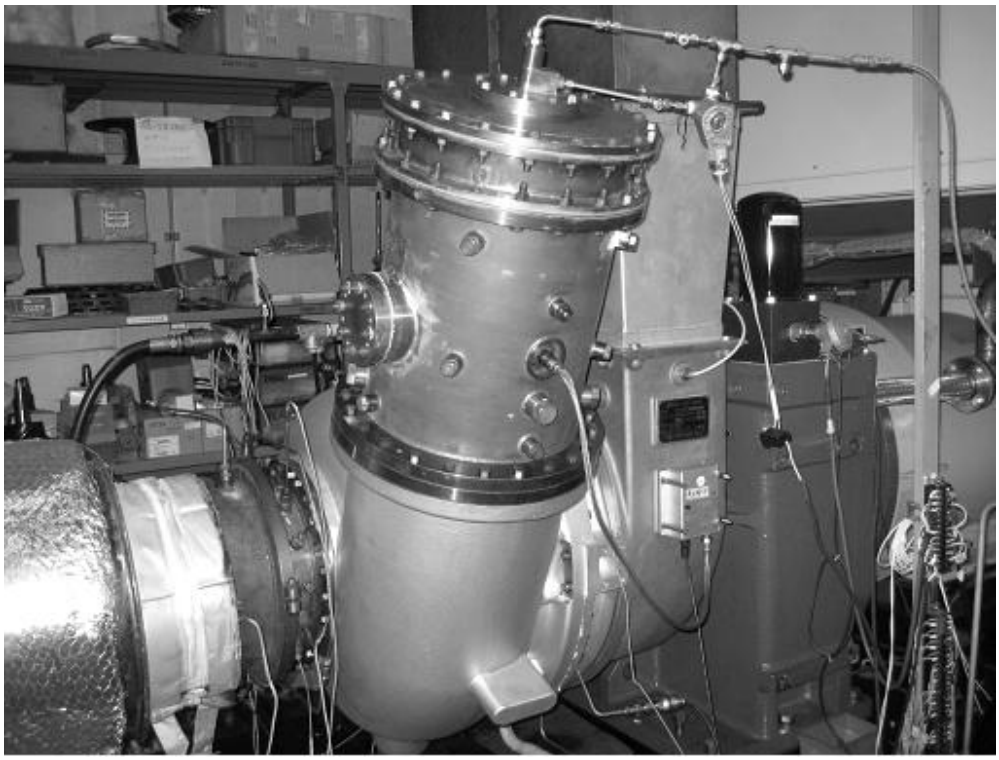

Fig. 12. Gas turbine engine testbed

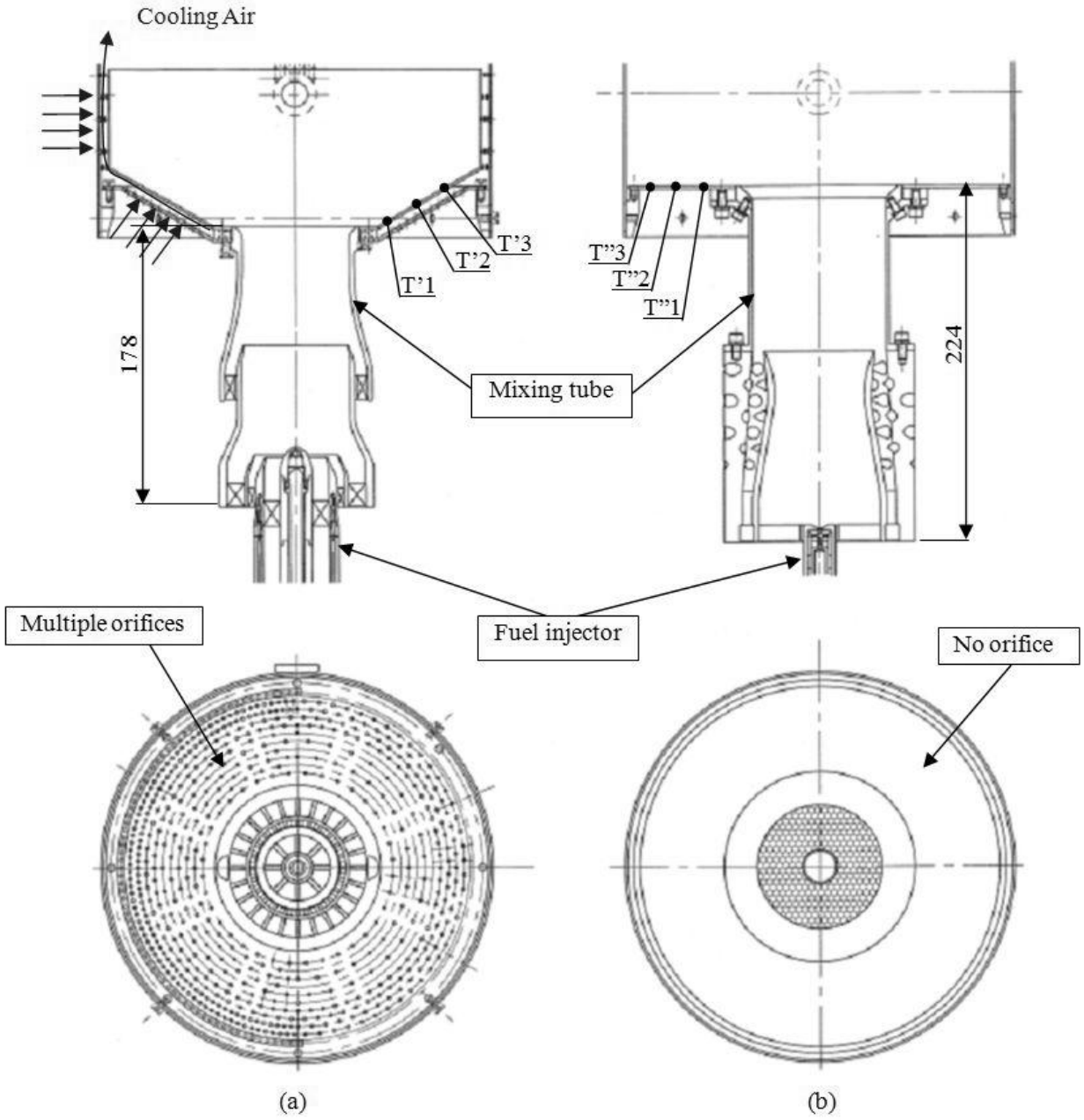

Fig. 13. Combustor inlet configurations: (a) production; (b) present

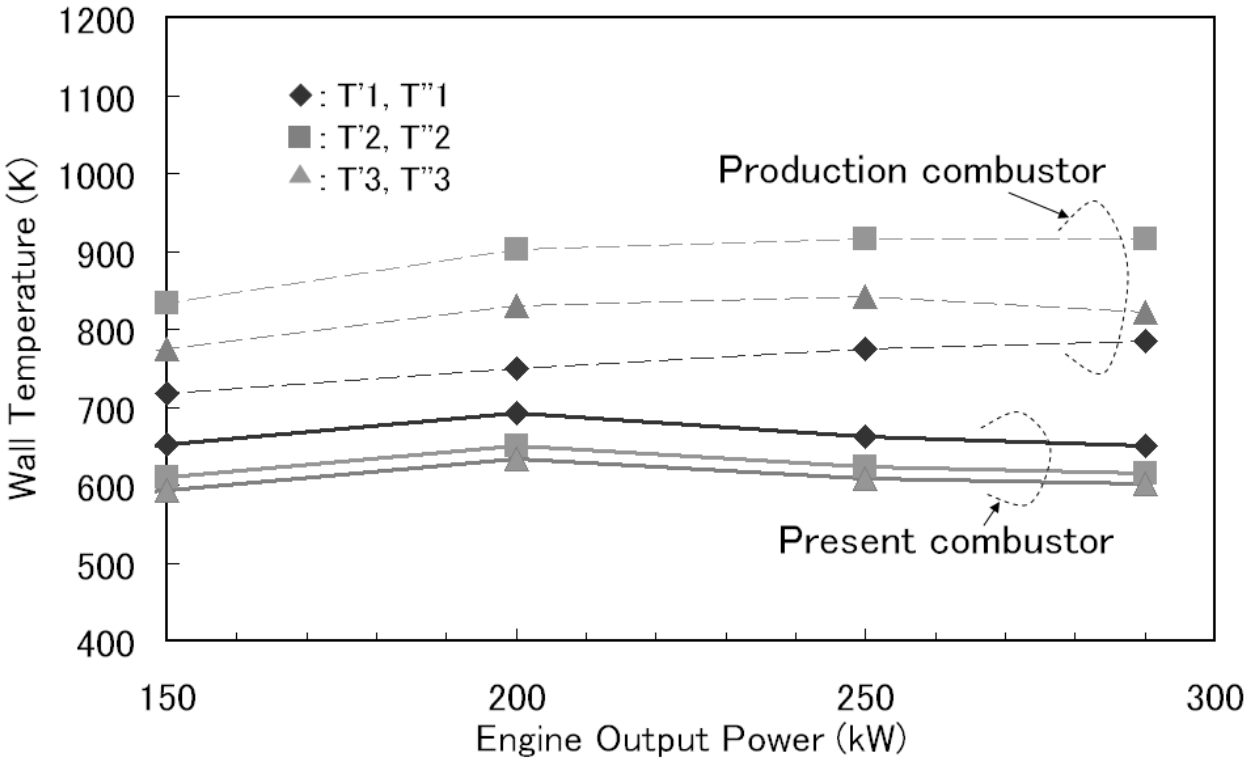

Fig. 14. Temperature at points on combustor inlet walls (see Fig.13 for location of measurement points T'1, T'2, T'3 and T"1, T" 2, T"3.)

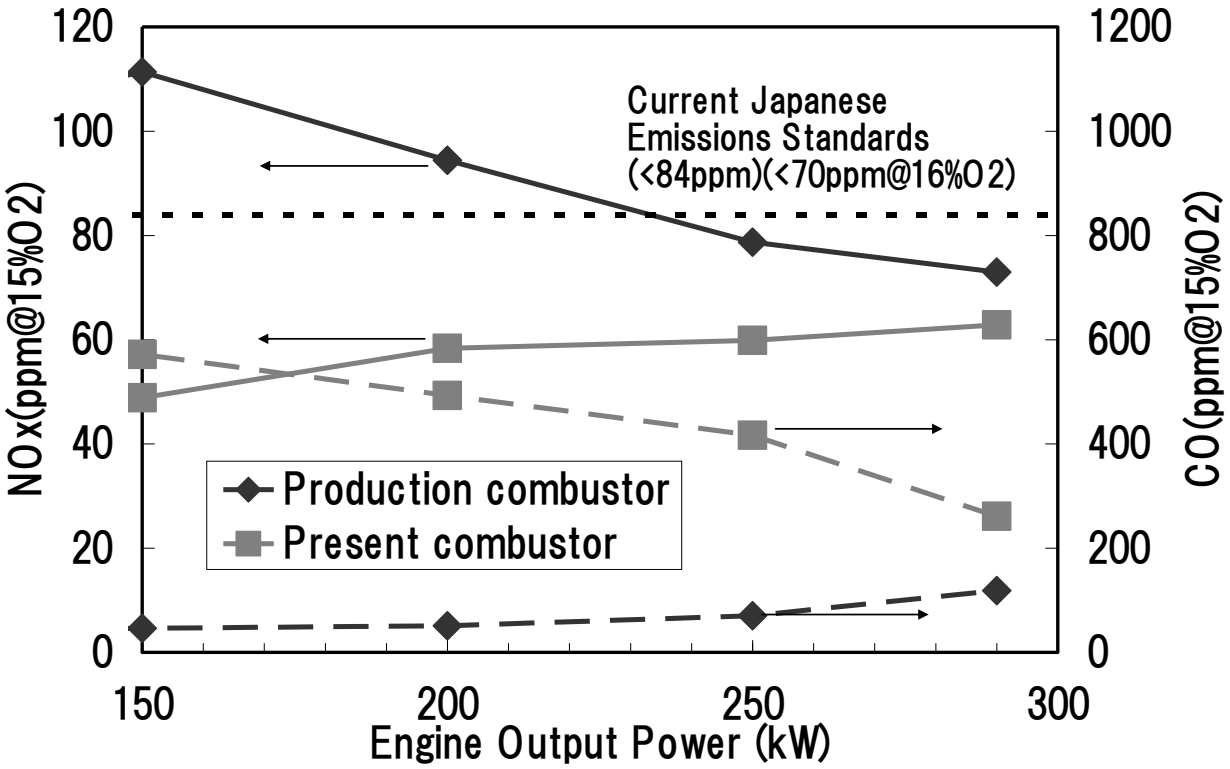

Fig. 15. NOx emissions under four conditions between half (150 kW) and full load (290 kW)

Table 1.
Atmospheric pressure combustion test conditions. (Nominal values at the fuel nozzle exit.)

Air flow rate (kg/s)	Air temperature (K)	Air velocity (m/s)	Equivalence ratio
0.625	473	48	0.56, 0.82, 1.08

Table 2.
Specifications of the gas turbine engine testbed.

Rated Power (kW)	Pressure Ratio	Air Flow Rate (kg/s)	Combustor Inlet Temperature (K)	Air velocity (fuel nozzle exit) (m/s)
290	4.01	2.5	473	48